# Laminar flame properties from spherically propagating premixed flames

HAMADI Alaa, ROQUE CCACYA Anthony, COUDORO Kodjo, CHAUMEIX Nabiha

ICARE-CNRS
Orleans, Loiret, France

## 1 Introduction

Alternative fuels for internal combustion (IC) engines have received increased interest as a result of increasingly significant environmental challenges and rigorous legislation. Natural gas, which is mainly composed of methane ($CH_4$), and hydrogen ($H_2$) are both regarded as environmentally friendly and possible alternative fuels. However, several difficult-to-solve issues prevent them from being extensively used in IC engines under mono-fuel conditions [1]. As a result, employing methane as the primary fuel and hydrogen as an additive fuel is seen to be a good strategy to compensate for each other's limitations.

To characterize the performance of methane/hydrogen/air mixtures, various properties must be studied. The burning velocity is an essential quantity in understanding flame. It serves as a significant metric for the validation of chemical reaction mechanisms. Because real flames are either curved or propagate through a complex flow field, the Markstein number or length, which measures the response of flame speed to stretch rate, is also useful to define flame behavior. Markstein number or length is a function of both the Zel'dovich number and the Lewis number [2]. The Zel'dovich number is a dimensionless number that quantitatively measures the activation energy. The correct determination of activation energy allows for the accurate calculation of Markstein length. Calculating the Markstein length and having values that are equivalent to measured ones allow one to estimate values for conditions that cannot be tested experimentally. Accordingly, the goal of this research is to explain the various methods for determining the activation energy by comparing theoretical Markstein length predictions with real measurements over a range of hydrogen-methane-air mixture compositions. For this, experiments are conducted out at a fixed $H_2$ content: 23% $H_2$ + 77% $CH_4$, at 1 bar for three distinct initial temperatures: 303 K, 333 K, 363 K, and at 2 bar for 303 K, both at equivalence ratios ranging from 0.7 to 1.3.

## 2 Experimental Set-up

The experiments are conducted using the spherical bomb facility at ICARE, Orléans. Prior publications describe the experimental setup and approach in detail ([3] and previous works). In brief, the spherical bomb consists of a 56-L spherical stainless-steel vessel equipped with 4 quartz windows (100 mm optical diameter). The equipment is heated to the required temperature by a heat transfer fluid, and the

Correspondence to: alaa.hamadi@cnrs-orleans.fr. 

thermal insulation guarantees uniform temperature distribution throughout the apparatus with a maximum deviation from the target value by ±1 K. Two tungsten electrodes are located along the sphere's diameter and are used to ignite the fuel–air mixtures. They are connected to a regulated high voltage discharge device, which generates a spark in the middle of the spherical reactor. The voltage and intensity discharge are measured using a high voltage and a current probe, allowing the energy given to the mixture to be determined. Before each experiment, the chamber is pumped down to less than 2 Pa. The gases are introduced directly into the vessel using the partial pressure approach. To reduce errors in the mixture preparation, pressures are monitored using capacitive manometers (MKS Baratron, Type 631, accuracy 0.2%) with varied full scales based on the needed pressure range (100 Torrs, 1000 Torrs and 15000 Torrs). Based on the precision of the capacitive manometers, the uncertainty in the equivalence ratio (φ) is around 1%.

The combustion process is monitored using two different diagnostics: pressure measurements using a piezo-electric pressure transducer (Kistler 601A coupled to a Kistler Type 5011B Charge Amplifier), and visualization and recording of the expanding flames using a Z-type Schlieren coupled with a high-speed camera (Phantom v1610, 25000 frames per second acquisition rate). The two diagnostics are synced by a TTL signal generated at the onset of the spark between the electrodes. This synchronization is required in order to link the pressure rise with the data acquired by rapid imaging. The pressure signal, in particular, is utilized to ensure that all measurements were taken under constant pressure conditions. The images are then processed to obtain the flame radius as a function of time (Canny method), from which the adiabatic unstretched gas speed of the burned gases relative to the flame, $S_b^\circ$, and the burned Markstein length, $L_b$, can be derived by solving the non-linear equation developed by Ronney and Sivashinsky [4].

$$(\frac{S_b}{S_b^\circ})^2 \cdot ln\left(\frac{S_b}{S_b^\circ}\right)^2 = -\frac{2L_b \cdot K}{S_b^\circ},$$

where $K$ is the stretch rate. The values $S_b^\circ$ and $L_b$ are determined as follows: (i) a pair of $S_b^\circ$ and $L_b$ values are chosen to start the optimization process; (ii) the non-linear equation is solved to obtain the radii predicted by the equation based on the values of the chosen $S_b^\circ$ and $L_b$; and (iii) these radii are compared to the experimental ones; and if they differ, a new set of $S_b^\circ$ and $L_b$ is chosen. A MATLAB code is developed to carry out this optimization process. In the data processing, the minimum and maximum radii are chosen to prevent the ignition effect and the hydrodynamic instabilities/radiation effects, respectively. The unburned gases' unstretched laminar flame speed is calculated from the continuity through $S_u^\circ = \rho_b S_b^\circ / \rho_u$, where $\rho_b$ and $\rho_u$ are the densities of the burnt and unburned mixtures, respectively. The densities of unburned and burned gases are calculated using Equilibrium-COSILAB [5].

The present study measures the laminar flame speeds and Markstein lengths at a fixed $H_2$ content: 23% $H_2$ + 77% $CH_4$ at 1 bar for three different initial temperatures 303 K, 333 K, 363 K, and at 2 bar for 303 K, both at equivalence ratios ranging from 0.7 to 1.3.

## 3 Methodology for Markstein length calculation

A Markstein length characterizes the effect of flame stretch on laminar flame speed. The theoretical model of Bechtold and Matalon [6] is used to evaluate the theoretical Markstein length by calculating the Markstein number ($Ma_{calc}$):

$$Ma_{calc} = \frac{L_u}{\delta_f} = \alpha - \frac{(\sigma - 1) * \gamma_1}{\sigma}$$

The constants are $\alpha = \gamma_1 + \beta \cdot (Le_{eff} - 1) \cdot \gamma_2$, $\gamma_1 = \frac{2 \cdot \sigma}{\sqrt{\sigma}+1}$, and $\gamma_2 = \frac{4}{\sigma-1}\{\sqrt{\sigma} - 1 - ln\frac{1}{2}(\sqrt{\sigma}+1)\}$. It should be noted that $\gamma_1$ and $\gamma_2$ are evaluated based on the thermal conductivity-temperature dependency i.e. $\lambda$=f(T).

Where Lu is unburned Markstein length, $\delta$f is the laminar-flame thickness, $\sigma = \frac{\rho_u}{\rho_b}$ is the expansion rate, $\beta = \frac{E_a \cdot (T_a - T_u)}{R \cdot T_a^2}$ is the Zel'dovich number with Ea the overall activation energy and R the gas constant, and Leeff appearing in the expression for $\alpha$ is the effective Lewis number defined by Addabbo et al. [7]:

$$Le_{eff} = 1 + \frac{(Le_E - 1) + (Le_D - 1) \cdot A}{1 + A}$$

where $A = 1 + \beta(\emptyset - 1)$; $\emptyset = 1$ at $\varphi$=1, $\emptyset = \varphi$ at $\varphi$<1 and $\emptyset = 1/\varphi$ at $\varphi$>1. The E and D subscripts reflect the excess and deficient reactants, respectively, for a certain equivalence ratio. There are many ways to calculate the Lewis number ($Le$) when dealing with blended fuels. They are adequately discussed in the work of Bouvet et al. [8]. The authors concluded that the Le volume-based approach has the potential to reproduce salient properties such as Markstein length. In light of this, the current study adopts this methodology.

As seen in the preceding equations, the computed Markstein number/length is heavily dependent on the zeldovih number, which in turn is dependent on the accuracy of the calculated activation energy. The activation energy can be retrieved from the analysis of the laminar burning rate sensitivity to the adiabatic flame temperature variation or from the thermal explosion theory. In flames theory, the $E_a$ is defined as the slope of the mass burning flux and the inverse adiabatic flame temperature at constant equivalence ratio ($\varphi$) and pressure (p), and can be empirically determined through:

$$E_a = -2 \cdot R \left[ \frac{\partial \ln(\rho_u \cdot S_L^\circ)}{\partial \left(\frac{1}{T_a}\right)} \right]_{\varphi,p}$$

Where $T_a$ is the adiabatic temperature.

Two common methods are applied in order to evaluate this differential. The first is accomplished by slightly varying the inert concentration as done by [8]. The second approach based on preheating the unburned gas is performed by adjusting the unburnt gas temperature as demonstrated by [9]. The latter is employed in the current article, although subsequent research will be conducted utilizing the former as well. The computation of the effective energy and reaction order using thermal explosion theory is thoroughly described in [10] and will not be duplicated here.

For the purpose of this work, the activation energy and Zel'dovich number are calculated using both theories and two different kinetic mechanisms GRI.03 [11] and Curran [12], which are widely validated against experimental data including hydrogen, methane, and their mixtures. Figure 1 represents an example of the activation energy and Zel'dovich number calculated for the 23% $H_2$ + 77% $CH_4$ mixture at P=1 bar and $T_{ini}$=363 K. As can be shown in Figure 1,a, the activation energy and Zel'dovich numbers calculated using the Flame theory are twice as large as those predicted using the explosion theory (Figure 1,b). The same observation is realized in all the studied mixtures and conditions. Additional sensitivity analyses will be conducted to fully comprehend the huge differences between the two theories.

After computing the Zel'dovich number, the Markstein length can be calculated ($L_u$=$M_{calc}$*$\delta_f$). The laminar-flame thickness has two definitions that are commonly used. The first one is defined by $\delta_f =$

$(\lambda/C_p)/(\rho_u S_L^\circ)$, where the ratio of thermal conductivity to heat capacity ($\lambda/C_p$) is assessed for the unburned gas mixture at the average temperature between the inlet and the adiabatic-flame temperature [13]. The second is defined by $\delta_f = (T_a - T_{ini})/(\partial T/\partial x)_{max}$ based on gradient theory [14], where $(\partial T/\partial x)_{max}$ is obtained from the temperature profile solution extracted from 1-D propagating flame-COSILAB simulations [5]. Figure 2 displays the 23% $H_2$ + 77% $CH_4$ mixture's unburned measured and calculated using the former flame thickness definition at various temperature and pressure conditions with the GRI.03 mechanism. The calculated results can satisfactorily predict the experimental results despite the theory used in calculating the Zel'dovich number as shown in Figure 2. Similar findings are obtained using Curran mechanism. However, when utilizing the second definition of flame thickness based on gradient theory, the calculated unburned Markstein length overpredicts the measured ones (Figure 3).

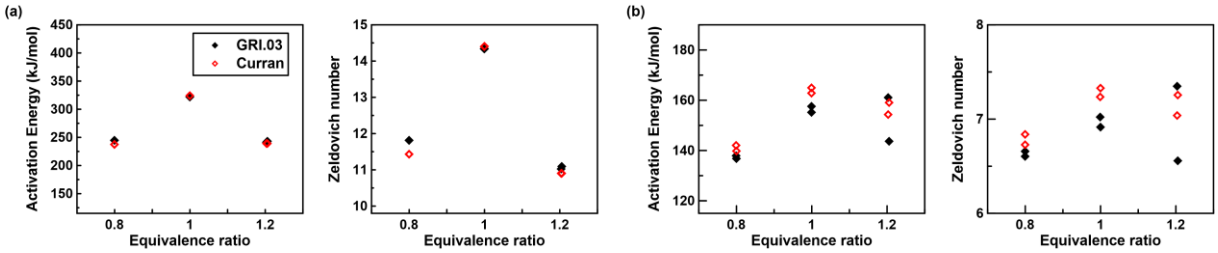


Figure 1: Activation Energy and Zel'dovich number as a function of equivalence ratio for the 23% $H_2$ + 77% $CH_4$ mixture at 1 bar and $T_{ini}$=363 K - (a) flame theory (b) thermal explosion theory

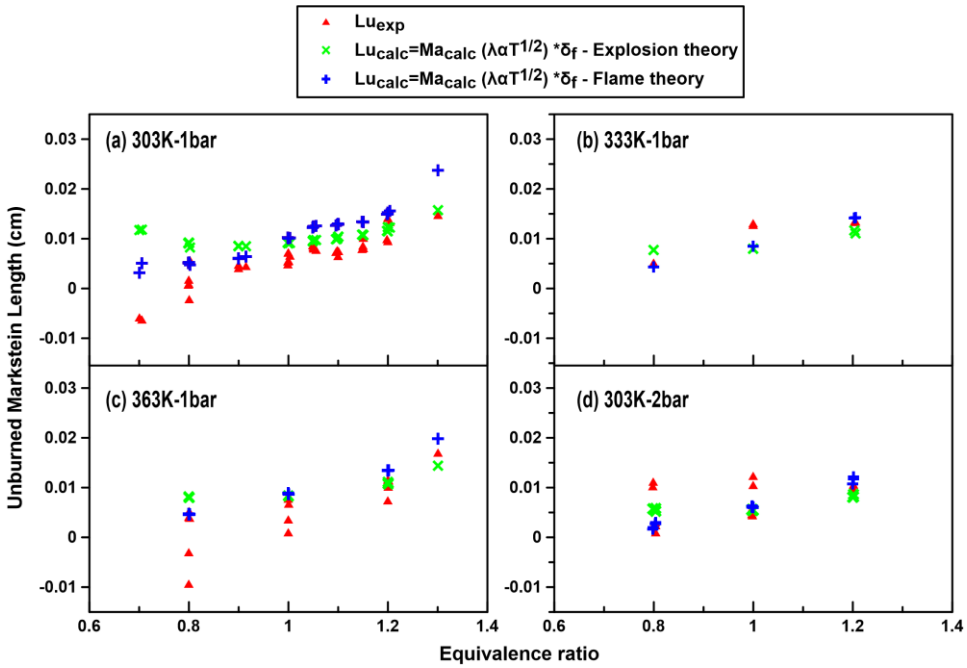


Figure 2: Unburned Markstein length as a function of equivalence ratio for the 23% $H_2$ + 77% $CH_4$ mixture. Here the flame thickness is defined by $\delta_f = (\lambda/C_p)/(\rho_u S_L^\circ)$.

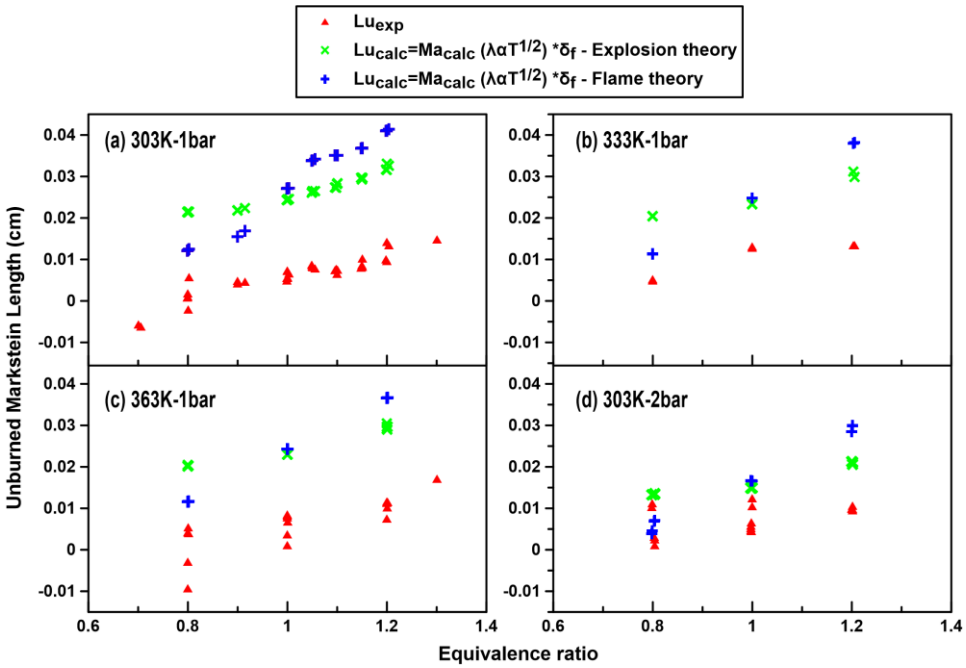


Figure 3: Unburned Markstein length as a function of equivalence ratio for the 23% $H_2$ + 77% $CH_4$ mixture. Here the flame thickness is defined by $\delta_f = (T_a - T_{ini})/(\partial T/\partial x)_{max}$

## 4 Conclusion

In this paper, the theoretical Markstein length for methane/hydrogen/air mixture with fixed $H_2$ content (23% $H_2$ + 77% $CH_4$) is estimated using the Bechtold and Matalon model over a wide range of temperature conditions (303 K, 333K, 363 K), two initial pressures (1 and 2 bar), and equivalence ratio range from 0.7 to 1.3. Because the predicted Markstein length is highly dependent on the Zel'dovich number and flame thickness definition, several theories and definitions are examined utilizing GRI.03 and Curran mechanisms. It was demonstrated that the flame thickness definition has a greater influence compared to the theory used to compute the activation energy (which is then used to calculate Zel'dovich number), as the Markstein length estimated with flame thickness based on kinetic analysis agrees with the experimental data more than the gradient flame thickness. Additional research on other fuels and models will be performed to validate this observation.

## Acknowledgment

This project has received funding from IRSN – INERIS - CNRS N°03 6325 project.

## References

[1] Okafor EC, Hayakawa A, Nagano Y, Kitagawa T. (2014). Effects of hydrogen concentration on premixed laminar flames of hydrogen–methane–air. Int. J. Hydrog. Energy; 39:2409–17.
[2] Gu XJ, Haq MZ, Lawes M, Woolley R. (2000). Laminar burning velocity and Markstein lengths of methane–air mixtures. Combust. Flame;121:41–58.
[3] Comandini A, Pengloan G, Abid S, Chaumeix N. (2016). Experimental and modeling study of styrene oxidation in spherical reactor and shock tube. Combust. Flame;173:425–40.
[4] Ronney PD, Sivashinsky GI. A. (1989). Theoretical Study of Propagation and Extinction of Nonsteady Spherical Flame Fronts. SIAM J. Appl. Math; 49:1029–46.

[5] COSILAB, The combustion simulation laboratory, Rotexo GmbH & Co., KG, Haan, Germany, 2009 Version 3.3.2 n.d.
[6] Bechtold JK, Matalon M. The dependence of the Markstein length on stoichiometry. Combustion and Flame 2001;127:1906–13. https://doi.org/10.1016/S0010-2180(01)00297-8.
[7] Addabbo R, Bechtold JK, Matalon M. (2002). Wrinkling of spherically expanding flames. Proc. Combust. Inst.; 29:1527–35.
[8] Bouvet N, Halter F, Chauveau C, Yoon Y. (2013). On the effective Lewis number formulations for lean hydrogen/hydrocarbon/air mixtures. Int. J. Hydrog. Energy; 38:5949–60.
[9] Ravi S, Sikes TG, Morones A, Keesee CL, Petersen EL. (2015). Comparative study on the laminar flame speed enhancement of methane with ethane and ethylene addition. Proc. Combust. Inst.; 35:679–86.
[10] Bane, Sally Page Moffett. (2010). Spark Ignition: Experimental and Numerical Investigation With Application to Aviation Safety; California Institute of Technology.
[11] GRI-Mech 3.0. Available online: http://www.me.berkeley.edu/gri_mech.
[12] Westbrook CK, Pitz WJ, Herbinet O, Curran HJ, Silke EJ. (2009). A comprehensive detailed chemical kinetic reaction mechanism for combustion of n-alkane hydrocarbons from n-octane to n-hexadecane. Combust. Flame; 156:181–99.
[13] Matalon M. (2009). Flame dynamics. Proc. Combust. Inst.; 32:57–82.
[14] Lafay Y, Renou B, Cabot G, Boukhalfa M. (2008). Experimental and numerical investigation of the effect of H2 enrichment on laminar methane–air flame thickness. Combust. Flame; 153:540–61.